JOURNAL OF GEOPHYSICAL RESEARCH, VOL. 93, NO. C6, PAGES 6774–6788, JUNE 15, 1988

# An Intercomparison of Four Mixed Layer Models in a Shallow Inland Sea

MICHAEL J. MCCORMICK

*Great Lakes Environmental Research Laboratory, NOAA, Ann Arbor, Michigan*

GUY A. MEADOWS

*Department of Naval Architecture and Marine Engineering, University of Michigan, Ann Arbor*

Four mixed layer (ML) models after *Denman* [1973] (KLD), *Garwood* [1977] (RWG), *McCormick and Scavia* [1981] (K), and *Thompson* [1976] (RT) were compared against an extensive water temperature data set collected in the central basin of Lake Erie during the summer of 1979. Results suggest that all four models are nearly equal in their ability to satisfactorily simulate surface water temperatures. However, if diurnal physical processes are of interest, then the model ability to simulate both the ML depth and the energy level associated with entrainment $dh/dt$ becomes crucial. While three of the models, KLD, RT, and RWG, were satisfactory in simulating the ML depth, only two of the models RT and RWG, were satisfactory in matching the energy levels seen in the entrainment spectra of $dh/dt$. This agreement suggests that the shear velocity $\Delta V$ entrainment scaling plays a critical role in the cycling of shallow depth mixed layers.

## INTRODUCTION

Thermal structure forecasting or mixed layer (ML) modeling has sustained attention over the past 3 decades because the same physics governing thermocline development controls the vertical transfer of mass and energy as well. Specific applications include predicting the density field for circulation models and estimating surface heat fluxes for climatology studies. Today uncertainties still exist in understanding thermal structure with even one-dimensional approaches, yet they need to be resolved before two-dimensional or fully three-dimensional modeling efforts can be confidently used.

The objectives of this work are (1) to evaluate four examples of existing one-dimensional ML models as to their applicability for use in shallow tideless seas and identify the best model if one exists, (2) to assess model predictability as a function of time and space, and (3) to assess model implications on vertical mixing.

This work comprises a comparison of four different ML models against data from Lake Erie. The 20-m-depth range of the central basin of Lake Erie provides a setting for indirectly evaluating the importance of shallow water effects on simulating the thermal structure. The Lake Erie data and the models will be discussed later.

The critical assumption that allows for one-dimensional treatment is that the local temperature profile is governed by local forces. Then in principle, if the surface wind stress, initial temperature profile, and surface heat flux are known, the resulting thermal structure is also. However, serious prediction errors can result if advective effects are ignored. For example, *De Szoeke* [1980] considered an idealized case of horizontally uniform temperatures in the open ocean and demonstrated that the persistence of even a weak curl in the wind stress was sufficient to produce fronts and upwelling and downwelling zones. *De Ruijter* [1983] showed how a uniform wind field but nonuniform surface heat flux in the horizontal could produce similar effects. Consequently, the ML depths in these areas would be poorly estimated by a strictly one-dimensional treatment. Here the horizontal transport of heat is clearly too major a component of the local thermal budget to be ignored. Similar conclusions apply to the Great Lakes.

In the Great Lakes region, storm cycles can be expected every 2–7 days [*Oort and Taylor*, 1969], and in consideration of storm size, the basin areas, and coastal effects, marked horizontal gradients in wind stress often result. When coupled with rotational effects, complex circulation patterns occur with coastal jets, upwellings, downwellings, internal seiching, etc. [e.g., *Bennett*, 1978; *Boyce*, 1974; *Mortimer*, 1974]. Hence regions subject to large-scale vertical motions, such as coastal areas prone to upwellings and downwellings, are poorly approximated by a one-dimensional model. In fact, because of the problem's nonlinear nature, even fully three-dimensional efforts have met with limited success in simulating the nearshore circulation and density field [*Allender and Saylor*, 1979; *Bennett*, 1977; *Simons*, 1976]. Yet the one-dimensional approach can still be a useful tool if (1) predictions are made far enough removed from coastal influences or, equivalently, in areas with minimum thermocline tilt or (2) predictions are made over time periods long enough to average out episodic events like upwellings and downwellings. The Lake Erie simulations were performed outside of the coastal boundary layer.

## PREVIOUS MODEL COMPARISONS

In contrast to the work done on thermocline modeling, relatively little has been done on head-to-head model intercomparisons. The more recent works of interest begin with *Thompson* [1976]. He compared three models against data from the ocean weather station November for 1967. One model assumed a constant ML depth, and the other two are a version of *Denman*'s [1973] and *Thompson*'s [1976] models. He found good correlation between predicted and observed sea surface temperature (SST) for all three models, with his model producing the best predictions of SST. However, in the wake of a plotting error pointed out in a later issue, Thompson's results were challenged by *Garwood and Camp* [1977]. Garwood and Camp suggested that the turbulent kinetic energy budget based models were more amenable to improved parame-

Copyright 1988 by the American Geophysical Union.

Paper number 8C0175.
0148-0227/88/008C-0175$05.00

terizations than models like Thompson's. In particular, they suggested that the excessive winter deepening problem of the Denman type model could be eliminated by reconsidering the dissipation parameterization, and they referenced appropriate works. *Thompson* [1977], acting on their suggestions, further modified the Denman model to accord *Elsberry et al.* [1976] for one case and *Gill and Turner* [1976] for yet another. The modifications improved model performance; however, the Thompson model still performed better than the other two.

*Le Saos and Mariette* [1981] compared the turbulence closure model of *Mellor and Durbin* [1975] and the integrated ML model of *Niiler* [1975]. The two models gave equivalent results except for the fall period when the Mellor and Durbin model overdeepened.

As extensive review of thermocline models was made by *Garwood* [1979]. He compared several models using a nondimensional framework described by a ML entrainment function, a ML depth function, and a stability function. Algorithms were constructed for each model in terms of these functions, and three-dimensional plots were made depicting model behavior. On the basis of these analyses the *Garwood* [1977] model and the previously mentioned Denman model [*Denman*, 1973; *Kraus and Turner*, 1967], modified to conform to either *Elsberry et al.* [1976] or *Gill and Turner* [1976], were found to be the most physically consistent. The *Thompson* [1976] model was not included in the comparison.

*Moen* [1981] reviewed thermocline development beginning with *Kraus and Turner* [1967] and included turbulence closure models and the *Pollard et al.* [1973] model. Although no simulations nor rigorous intercomparisons were made, their theoretical differences were clarified by deriving each model from the same basic equations, using consistent notation throughout.

Finally, *Martin* [1985] compared two turbulence closure models of *Mellor and Yamada* [1974, 1982] and two integrated ML models of *Niiler* [1975] and *Garwood* [1977]. Examination of Martin's Table 4, showing the difference between model-predicted and observed mean monthly SST for ocean weather stations November and Papa for 1961, suggests the Garwood model to be the most accurate of the four. It equalled or exceeded the performance of the other models for all but 2 months at each station (April and September at November, October and November at Papa). However, with different data sets or better data, different conclusions may be drawn (P. J. Martin, personal communication, 1987). Nonetheless, from these studies the *Garwood* [1977], *Thompson* [1976], and possibly the modified *Denman* [1973] models emerge as reasonable candidates for thermocline prediction.

## The Models

In general, there are four approaches to calculating thermal structure [*Niiler and Kraus*, 1977]: (1) turbulence closure models, (2) deterministic solutions, (3) eddy diffusion models, and (4) integrated ML models. All attempt to describe the evolution of the temperature field either by direct solution or by a combination of parameterization and simplification of the momentum, thermal, and turbulent kinetic energy equations through physically based arguments on the mixing processes. The four approaches have evolved from their treatment of the Reynolds terms.

First, turbulence closure models [e.g., *Mellor and Yamada*, 1974, 1982; *Mellor and Durbin*, 1975; *Zeman and Lumley*, 1976; *Kundu*, 1980] solve for the Reynolds terms through higher-order turbulence terms. The resulting triple-correlation products require additional assumptions and coefficients that must be empirically defined in order to solve the equations. *Martin* [1985] has shown that these models are not significantly better than the simpler integrated ML type models. More importantly, the mixing mechanism (i.e., mix if the Froude or Richardson number is greater than a critical value) is similar to two of the models used in this study [*Clancy and Pollak*, 1983], and since this mixing criterion is the major factor determining ML depth, turbulence closure models will not be considered here.

Second, deterministic solutions calculate the Reynolds terms directly and have been attempted by *Deardorff* [1970]. This approach requires very fine spatial and temporal resolution of the dependent variables as well as of the initial conditions, but it is too time consuming and costly to be of practical interest.

Third, the eddy diffusion or "K" models are based on the thermal energy equation and on the assumption that the Reynolds terms can be expressed according to Fick's law. It is a bold assumption to assume a local relationship between mean scalar fields and eddy fluxes [*Davis*, 1983] because theoretical principles suggest that none exists [*Batchelor and Townsend*, 1956; *Roberts*, 1961]. Nonetheless, this has been a popular approach [e.g., *Kent and Pritchard*, 1959; *Pacanowski and Philander*, 1981; *Sundaram and Rehm*, 1973; *McCormick and Scavia*, 1981; *Walters et al.*, 1978] since *Munk and Anderson* [1948] first used it to describe thermocline formation. However, this approach has been criticized on two accounts. The physical basis for K models stems from *Taylor*'s [1931] work where the eddy transfer coefficient is formulated in terms of a stability parameter (Richardson number). The data set [*Jacobsen*, 1913] used in formulating the Richardson number has been criticized by *Woods* [1977] as being too limited (i.e., data were taken in the Kattegat at eight levels separated by 2.5 m) and thus is too weak a foundation for building models. The second objection is concerned with the lack of a meaningful scale dependence. For example, *Hoeber* [1972] noted in the tropical North Atlantic an order of magnitude increase in the eddy viscosity with a 1-m/s increase in the wind speed. This sensitivity to environmental conditions limits confidence in vertical transport predictions. Although these criticisms are severe, the continuing popularity of the approach dictates their inclusion if for no other reason than comparative purposes. The *McCormick and Scavia* [1981] model will be used to represent this model category because of its success in simulating other Great Lakes data.

The fourth type of thermocline model originated with *Kraus and Turner* [1967] and stems from assumptions based on observations of upper ocean structure. Discontinuities in temperature and dissolved components are observed across the air-sea interface and across the base of the ML. Within the surface ML these distributions are, however, relatively uniform and can be represented as bulk or integrated variables, behaving as if the upper layers are responding as a "slab" to the external forcing. This model type may be further subdivided into two classes based upon the physical assumptions by which water is entrained and the ML deepens. They are turbulent erosion models (TEM) and dynamic instability models (DIM) [*Cushman-Roison*, 1981]. Entrainment in the TEM approach is proportional to the wind energy input to the water column minus the work performed in overcoming the buoyancy forces at the ML base. This is the *Kraus and Turner* [1967] model type. The DIM, on the other hand, parameterizes deepening events to occur when the mean flow becomes

unstable. This approach originated with *Pollard et al.* [1973]. Instabilities in the mean flow are assumed to be shear generated with inertial oscillations as the shear source.

On the basis of the preceding discussion, the following four models will be used in this study: (1) *McCormick and Scavia* [1981], (2) *Denman* [1973], (3) *Thompson* [1976], and (4) *Garwood* [1977]. The Denman and Garwood models will be referred to by the authors' initials, i.e., KLD and RWG, respectively. The Thompson model will be identified by the letters "RT." in reference to Rhines and Thompson (R. O. R. Y. Thompson, personal communication, 1987), and the McCormick and Scavia model will be referred to hereinafter as the K model. For convenience each model will be briefly described.

### *K Model*

In the Great Lakes the *McCormick and Scavia* [1981] model was successful in describing lake-wide average temperatures in Lake Ontario. Formulation of the eddy diffusivities is empirically based and similar to *Kent and Pritchard*'s [1959] work, a relatively popular model. The model is described by the following two equations:

$$\partial T/\partial t = \frac{\partial}{\partial z}\left(K\frac{\partial T}{\partial z}\right) + \frac{1}{\rho_0 C_p}\frac{\partial R}{\partial z} \qquad -H \le z \le 0 \tag{1}$$

$$\begin{aligned} K &= (U_*)^3/(\beta g \alpha k^2 z^2\ \partial T/\partial z) \qquad z \ge -h_T \\ K &= K(z = -h_T) \qquad z < -h_T \end{aligned} \tag{2}$$

where

- $T$ temperature;
- $t$ time;
- $z$ vertical coordinate, positive upward;
- $R$ penetrative component of solar energy, positive in the negative $z$ direction;
- $g$ gravitational constant;
- $C_p$ specific heat at constant pressure;
- $\alpha$ volumetric expansion coefficient, equal to $-(1/\rho_0)(\partial\rho/\partial T)$;
- $\rho_0$ reference density;
- $H$ lake depth;
- $h_T$ depth of the minimum thermocline diffusivity;
- $U_*$ friction velocity of water, equal to $(|\tau|/\rho_0)^{0.5}$;
- $\tau$ surface wind stress vector, equal to $\rho_a C_d |W| W$;
- $\rho_a$ air density;
- $C_d$ drag coefficient at 10 m;
- $W$ wind vector;
- $k$ Von Karman's constant, equal to 0.4;
- $\beta$ empirical coefficient.

These equations are solved subject to the boundary conditions

$$K\left.\frac{\partial T}{\partial z}\right|_{z=0} = \frac{Q}{\rho_0 C_p} \qquad \left.\frac{\partial T}{\partial z}\right|_{z=-H} = 0 \tag{3}$$

where $Q$ is the surface heat flux and no heat is transferred across the sediment-water boundary.

### *KLD Model*

This model is a generalization of the Kraus-Turner model whereby routine meteorological data are input rather than idealized distributions of the forcing functions [see *Denman and Miyake*, 1973]. The model's historical nature makes its inclusion worthwhile despite the known deficiency of excessive winter deepening. Attempts to remedy this problem suggest that dissipation mechanisms like those of *Elsberry et al.* [1976] or *Stevenson* [1979] need to be included. For the shallow environment of Lake Erie, however, no attempt was made to explicitly account for dissipation.

The KLD model and ambient diffusion below the ML are described by (4)–(6).

$$\frac{dT}{dt} = \frac{2}{h^2}\left[\frac{Qh + R(0)h - 1}{\rho_0 C_p}\int_{-h}^{0} R(z)\,dz - \frac{m\rho_a C_d W^3}{\alpha g \rho_0}\right] \tag{4}$$

$$\Lambda(dh/dt) = \left\{2m\rho_a C_d W^3/\alpha g\rho_0 + \left[2\int_{-h}^{0} R(z)\,dz - h[Q + R(0) + R(-h)]\right]\Big/\rho_0 C_P\right\}\{h[T - T(-h)]\}^{-1} \tag{5}$$

$$\partial T(z)/\partial t = K\frac{\partial^2 T(z)}{\partial z^2} + \frac{1}{\rho_0 C_P}\frac{\partial R}{\partial z} \qquad -H < z < -h \tag{6}$$

where $W$ is the mean wind speed at 10 m, $m$ is the empirical constant, and

$$\Lambda = 1 \qquad dh/dt > 0$$

$$\Lambda = 0 \qquad dh/dt \le 0$$

Equation (4) describes the temporal behavior of the ML temperature $T$ over the ML depth $h$. Equation (5) expresses the entrainment relation for ML deepening, and it is constrained by the $\Lambda$ function to avoid the physically meaningless situation of negative entrainment. Equation (6) is used to describe ambient mixing below the surface ML. This mechanism has also been implemented in the RT and RWG models.

### *RT Model*

If the momentum equations are integrated over the ML depth and the total shear stress at the base of the ML, $\tau(-h)$, is used to accelerate the entrained fluid to velocity $V$, that is, $(\tau(-h) = V\ \partial h/\partial t)$, then the momentum equations become

$$d(hu)/dt - fhv = \tau^x/\rho_0 \tag{7}$$

$$d(hv)/dt + fhu = \tau^y/\rho_0 \tag{8}$$

where $\tau^x$ and $\tau^y$ are the eastward and northward components, respectively, of the surface wind stress vector $\tau$, and similarly, $u$ and $v$ are the $x$ and $y$ components of the inertial current $V$, and $f$ is the Coriolis parameter. These last two equations coupled with

$$\frac{\partial T}{\partial t} = \frac{1}{\rho_0 C_p}\frac{\partial R}{\partial z} \tag{9}$$

form the model first identified with *Pollard et al.* [1973]. The hypothesis used to close these equations is that the mean flow remains marginally stable. This suggests that the Froude number $F$ be unity throughout the ML [*Thompson*, 1979].

$$F = \frac{u^2 + v^2}{gh\Delta\rho/\rho_0} = 1 \qquad -h \le z < 0 \tag{10}$$

*Thompson* [1976] further modified this model by assuming zero momentum below the ML. This is a reasonable approximation since it is the current shear, not magnitude, which controls deepening. The model's main attraction is that no arbitrary coefficients are required for calibration. Because there are fewer sinks for momentum than for energy, the RT model is physically attractive provided that the momentum balance can be described in a one-dimensional framework.

*RWG Model*

The RWG model [*Garwood*, 1977] contains features of both the KLD and RT models whereby entrainment can occur from turbulent erosion and shear instability mechanisms. The model is unique in that Garwood recognized the nonisotropic nature of ML turbulence and hence decomposed the turbulent kinetic energy (TKE) budget into horizontal and vertical components. Equations (11)–(14) describe the model.

$$0 = m_3 u_*^3 - \left[\frac{(\Delta u)^2 + (\Delta v)^2}{2}\right]\frac{\partial h}{\partial t} - m_2(\xi - 3w'^2)\xi^{0.5} - \tfrac{2}{3}(m_1\xi^{1.5} + m_5 fh\xi) \quad (11)$$

$$0 = -\alpha g\frac{h}{2}\Delta T\frac{\partial h}{\partial t} + \Phi + m_2(\xi - 3w'^2)\xi^{0.5} - \tfrac{1}{3}(m_1\xi^{1.5} + m_5 fh\xi) \quad (12)$$

$$\Phi = -\frac{\alpha g h}{2\rho_0 C_p}(Q + R(0) + R(-h) + \frac{\alpha g}{\rho_0 C_p}\int_{-h}^{0} R(z)\,dz \quad (13)$$

$$\alpha g h \Delta T\ \partial h/\partial t = m_4 \xi w' \quad (14)$$

where $\Delta T = T - T(-h)$ and $\xi = u'u' + v'v' + w'w'$, which is twice the total TKE, with the primes denoting the fluctuating component of the velocity. A suitable time average is implied in all terms involving products of fluctuating quantities. As in (5), if $\partial h/\partial t < 0$, then the buoyancy flux is determined solely by the value of $\Phi$. The velocity jump, $\Delta u$ and $\Delta v$, in (11) is determined the same way as in the RT model, by using the ML momentum equations (7) and (8). Both *Martin* [1985] and *Garwood* [1977] ignored the shear TKE production term (and thus the need to worry about momentum) in their simulations, but it is retained here in order to better describe strong shear (i.e., storm) induced deepening [*Adamec et al.*, 1981]. Finally, temperatures below the ML are described by (6) in the same way as in all of the preceding models.

The constants $m_1$ and $m_5$ scale dissipation, $m_2$ scales the partitioning of TKE between the horizontal and vertical, $m_3$ scales the surface flux of TKE, and $m_4$ scales the energy flux at the ML base. Following *Garwood* [1977] and *Martin* [1985], $m_1 = m_2 = m_4 = 1.0$ and $m_3$ and $m_5$ are adjusted to obtain a good data fit. Finally, $\partial h/\partial t$ and all terms containing $w'$ are set equal to zero when the ML is shallowing [*Martin*, 1985].

## The Data

*Water Temperatures*

Water temperature data were collected at four sites in Lake Erie, by the Great Lakes Environmental Research Laboratory (NOAA) in Ann Arbor, Michigan, from early May to late October 1979. The stations are identified in Figure 1, and their numbers (9, 11, 19, and 21) will be frequently referred to in the discussion of the model results. Stations 9 and 11 form the westernmost locations situated approximately 20 km offshore and about 40 km apart in a north-south direction. Stations 19 and 21 are the eastern data stations. When viewed from above, the four stations roughly outline a 100 km by 40 km rectangle whose long axis parallels the lake's.

Approximately 150,000 total observations of water temperature were recorded during this period. At each site 10 thermistors were placed 1–2 m apart on a fixed mooring. The shallowest thermistor was located no closer than 4 m from the surface, while the deepest thermistor was fixed about 3 m above the bottom. Station depths ranged from 20 to 23 m. The actual thermistor depths and a description of the temperature data can be found in the work of *Saylor and Miller* [1983].

None of the water temperatures in the NOAA data set included surface observations. Therefore in order to form a complete data base for model comparisons, the surface water temperature at each thermistor string was assumed to be equal to the SST recorded by nearby meteorological buoys. The buoys were deployed by the National Water Research Institute (NWRI) in Burlington, Ontario, as part of a joint research effort with NOAA. The meteorological buoy locations are shown in Figure 1 and their data will be described shortly. In all there were six buoys deployed in Lake Erie. Three of these buoys were used to estimate SST for the NOAA stations. For NOAA stations 9, 11, 19, and 21 the NWRI stations 24, 26, 47, and 47, respectively, were used to estimate SST. Note that NWRI station 47 was used for both of the NOAA stations 19 and 21. Figures showing the temperature isotherms for Lake Erie will be shown later with the model simulations.

*Meteorological Data*

In Lake Erie, meteorological data were collected at hourly intervals at six buoys deployed by NWRI (see Figure 1). At each buoy, wind speed, wind direction, air temperature, vapor pressure, and SST measurements were collected. In addition, two of the six stations (26 and 47) were equipped with integrating pyranometers to measure solar irradiance. The pyranometer data were available from early June through late September, and there were varying time periods when one or both pyranometers did not function. During these periods the data gaps in solar irradiance were filled by a model after *Cotton* [1979]. Model estimates were used only if data from neither pyranometer were available. No estimates of overwater cloud cover were available from the NWRI data set; therefore cloud data from Cleveland, Ohio, were used in its place.

Meteorological data from the three NWRI stations that were closest in distance to the four NOAA stations were used in the model simulations. Figures 2 and 3 show all of the meteorological data used to force the models. The vapor pressure data were converted to dew point temperature using standard methods.

## Surface Energy Balance and Model Implementation

The surface boundary condition common to the models is related to the surface energy balance according to

$$E_s = Q + I_0 \qquad Q = L_n - H_s - H_L \quad (15)$$

where

- $E_s$ surface energy balance (in watts per square meter);
- $I_0$ net incoming shortwave radiation, equal to $(1 - A)I_s$;
- $I_s$ incoming shortwave radiation;
- $A$ surface albedo, equal to 0.045/cos (solar zenith angle) with a maximum albedo of 1 [*Pinsak and Rodgers*, 1981];
- $L_n$ net longwave radiation;
- $H_s$ sensible heat loss;
- $H_L$ latent heat loss.

The net incoming shortwave radiation $I_0$ is the only component of (15) that can penetrate beyond the surface layer and

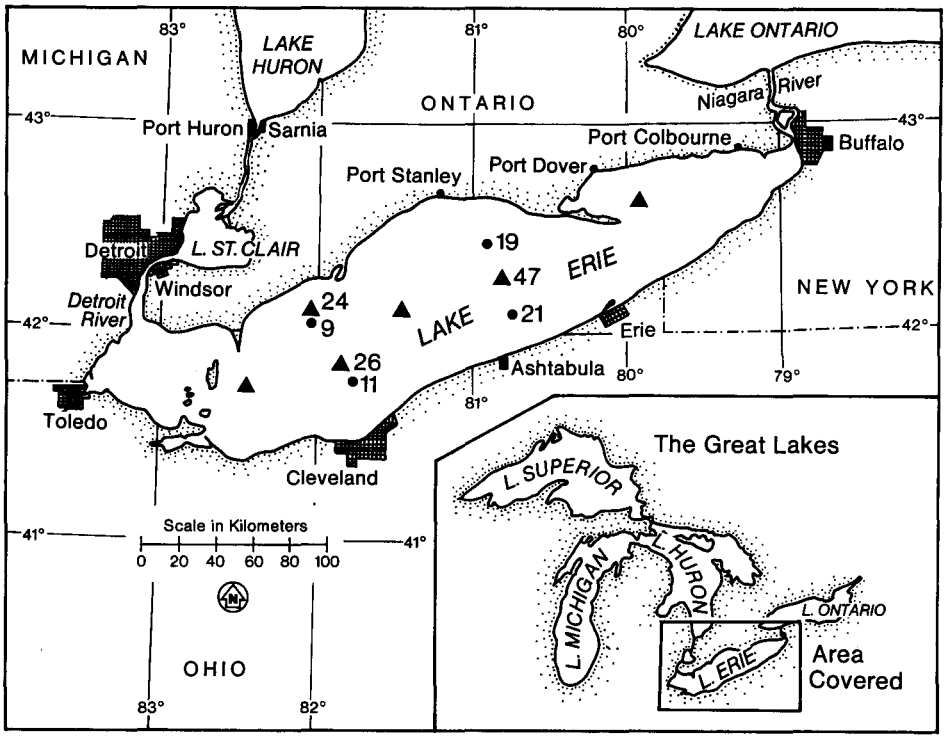


Fig. 1. Locations of NOAA thermistor string moorings (solid dots) and National Water Research Institute (NWRI) meteorological buoys (solid triangles) in Lake Erie, 1979.

passively heat water at depth. Solar heating at depth was approximated by

$$I(z) = I_0[0.45 \exp(\varepsilon_1 z) + 0.55 \exp(\varepsilon_2 z)] \quad (16)$$

The leading coefficients in (16) reflect the relative contribution of visible and infrared radiation, respectively, to $I_0$ [*Ivanoff*, 1977]. Similarly, the extinction coefficients $\varepsilon$ account for absorption by water on these energy bands. Extinction values of 0.28 $m^{-1}$ and 2.85 $m^{-1}$ were used, respectively.

The longwave radiation $L_n$ was calculated after *Wyrtki* [1965], and the sensible and latent heat fluxes $H_s$ and $H_L$ were calculated from bulk aerodynamic equations.

Each of the four models was integrated with a 15-min time step over a constant grid interval of 1 m and solved by an explicit numerical scheme. Program flow begins with inputting meteorological data and interpolating linearly in time to the current time step from which the bulk aerodynamic coefficients for heat and momentum are calculated. The bulk transfer coefficients for sensible and latent heats were assumed to be equal. The wind stress vector is calculated next with a stability dependent drag coefficient after *Schwab* [1978]. This method is based on the work of *Businger et al.* [1971], and the program is documented by *Schwab et al.* [1981]. This calculation is followed by the calculation of the surface heat flux and internal radiative heating.

The temperature profile is then integrated in accord with the physics of the respective models and then checked for hydrodynamic instabilities using an equation of state after *Pickett and Herche* [1984]. If any instabilities are present, they are removed by mixing the layer in question with lower layers, in a heat-conserving manner, until the instability is eliminated. The RWG model, however, employs a slightly different mechanism but accomplishes the same result by assuming that at any time step an instability can be removed by mixing with the next lower layer only.

The optimal model coefficients were determined by estimating which parameter values gave the lowest root-mean-squared error (RMSE) between the predicted and observed SST for Lake Erie. To find the optimal model parameters, numerous simulations were run with each model. The single coefficient $\beta$, used in the K model, was varied, and a value of 0.02 $m^{-1}$ was found to give the best agreement with data.

There are two possible tuning parameters in the KLD model. The first $m$ is the original model parameter [*Denman*, 1973] which controls the transfer rate of TKE into potential energy. The second parameter was suggested by *Thompson* [1977] to limit the excessive deepening of the mixed layer, seen in oceanic simulations, by removing energy through dissipation. For the application described herein the need for this particular mechanism was not demonstrated. Perhaps with the deeper ML depths found in the other Great Lakes this would not have been true. However, in any case it is difficult to envision its being important in Lake Erie because of the shallow lake depth. Hence simulations were performed with KLD, varying only $m$, and the optimal value was found to be 0.0012. This was the same value used by *Denman and Miyake* [1973] in the northeast Pacific Ocean.

Practically speaking, the RT model has no adjustable parameters. The closure hypothesis used to balance thermal and mechanical energy inputs is that the Froude number be unity at the base of the ML. The model simulations were performed as such for each lake station.

Following *Martin* [1985] and *Garwood* [1977], three of the five parameters, $m_1$, $m_2$, and $m_4$, used in the RWG model were held constant at unity. The remaining two, $m_3$ and $m_5$, scale the surface flux of TKE and dissipation, respectively. The

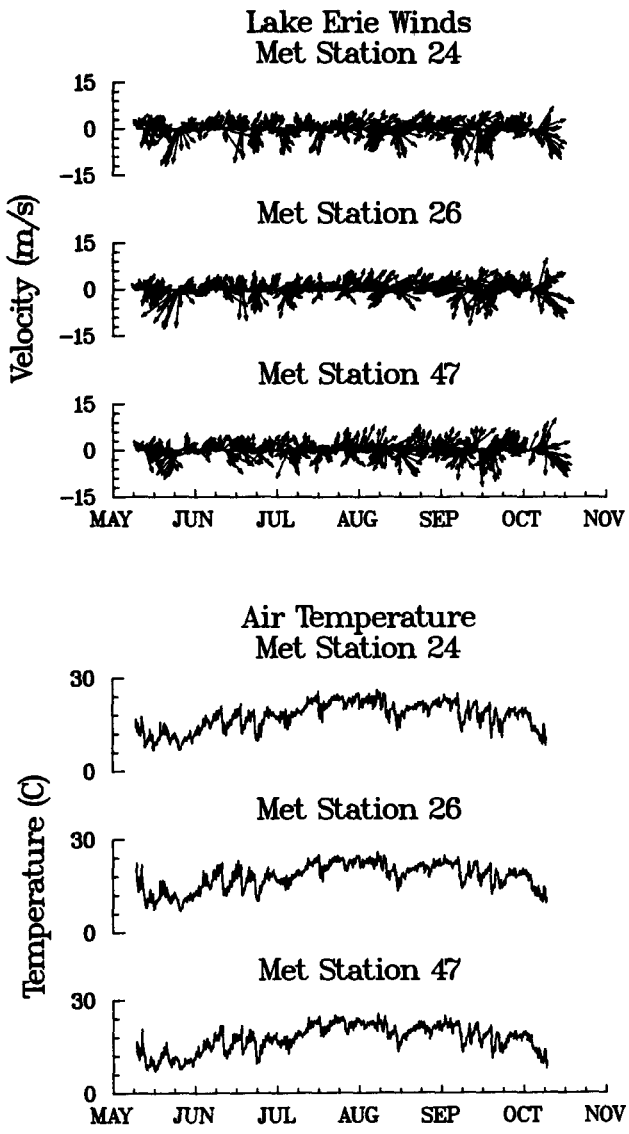


Fig. 2. Vector averaged wind velocities (6 hours) and hourly air temperatures from the three NWRI buoys used in the model simulations.

values that gave the best agreement with data were $m_3 = 4.5$ and $m_5 = 4.6$. These also were the same values that *Martin* [1985] used to simulate temperatures in the North Pacific; however, recall that this version of RWG includes the shear production term of TKE which was absent in Martin's simulations.

## Model Simulations

### *Idealized Forcing Experiments*

To help better understand and interpret the model simulations of the lake data, each model was tested under idealized conditions for wind deepening, heating, and cooling. The models were run using the same coefficients determined by the calibration exercise and with a uniform 1-m grid extending to a maximum depth of 100 m. The operational definition of ML employed here is the same as *Martin*'s [1985], that is, $h$ is the depth where $|T - T(-h)| = 0.1°C$.

The wind deepening experiment was run for 48 hours. The initial conditions were a water column with a linear temperature gradient of 0.05°C/m, a ML depth of 1 m, a SST of 23°C, and no surface heat flux. Five different wind speeds were used and held constant for the duration of the experiment. The results are shown in Table 1. For three of the models, RT, KLD, and RWG, the ML depth responded linearly to changes in the wind speed. A doubling of the wind speed from 5 to 10 m/s and from 10 to 20 m/s resulted, in each case, in an approximate doubling in ML depth. Two other features are noteworthy. First, the K model, using the operational definition of ML depth, did not respond to increases in wind speeds beyond about 5 m/s. The reason was that the calculated diffusion coefficients reached the maximum value allowed by the numerical stability criterion, and once the maximum is reached, the model is insensitive to further increases in wind speed.

The second feature concerns the RT model performance. The model's rapid response to the wind stress and the rapidity with which the entrainment process is arrested are well illustrated under conditions of constant unidirectional winds. Under these idealized conditions, deepening stops in half of an inertial period or, at these latitudes, in about 8.5 hours.

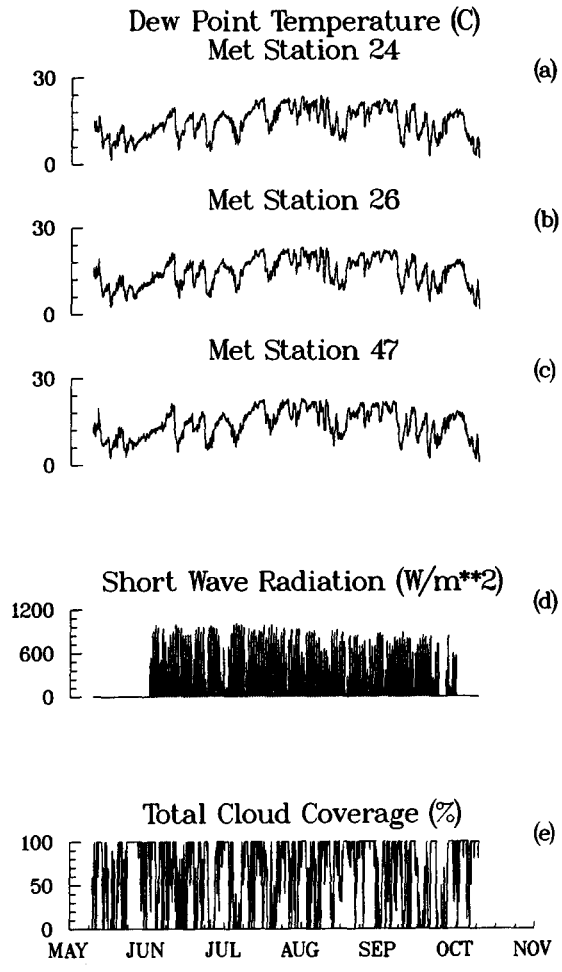


Fig. 3. (*a*) Hourly dew point temperature at station 24, (*b*) hourly dew point temperature at station 26, (*c*) hourly dew point temperature at station 47, (*d*) hourly measured solar irradiance, and (*e*) cloud coverage.

TABLE 1. Idealized Forcing Experiments Showing Model Responses in ML Temperature and Depth to Wind Deepening, Surface Heating, and Surface Cooling

| | ML Temperature, °C | | | | ML Depth, m | | | |
|---|---|---|---|---|---|---|---|---|
| | RWG | RT | KLD | K | RWG | RT | KLD | K |
| | | | *Wind Deepening* | | | | | |
| Wind, m/s | | | | | | | | |
| 1 | 22.94 | 22.92 | 22.90 | 22.86 | 3 | 3 | 4 | 6 |
| 5 | 22.67 | 22.72 | 22.58 | 22.44 | 14 | 12 | 17 | 8 |
| 10 | 22.31 | 22.45 | 22.14 | 22.44 | 28 | 23 | 35 | 8 |
| 15 | 21.95 | 22.15 | 21.69 | 22.44 | 43 | 35 | 53 | 8 |
| 20 | 21.59 | 21.85 | 21.23 | 22.44 | 57 | 47 | 71 | 8 |
| | | | *Heating* | | | | | |
| Heat flux, W/m$^2$ | | | | | | | | |
| 125 | 10.63 | 10.66 | 10.46 | 10.77 | 20 | 18 | 26 | 4 |
| 250 | 11.70 | 11.86 | 11.70 | 11.57 | 14 | 12 | 13 | 3 |
| 500 | 15.12 | 14.86 | 16.29 | 13.20 | 8 | 9 | 6 | 2 |
| | | | *Cooling* | | | | | |
| Heat flux, W/m$^2$ | | | | | | | | |
| −125 | 19.34 | 19.37 | 19.32 | 19.08 | 33 | 29 | 35 | 29 |
| −250 | 18.93 | 18.95 | 18.94 | 18.72 | 42 | 37 | 40 | 40 |
| −500 | 18.31 | 18.33 | 18.33 | 18.17 | 55 | 50 | 51 | 55 |

Experiment durations were 48, 120, and 120 hours, respectively. RWG, RT, KLD, and K refer to models.

Both the KLD and RWG models show similar responses to wind deepening. The deepening rate begins quickly in both models, but not as fast as in RT, and then decreases in magnitude as time passes. The final ML depth in the 15-m/s case was 42 m for RWG and 53 m for KLD. The deeper ML in KLD results from its having fewer energy sinks than RWG and thus more energy available for entrainment and a deeper ML.

Three different test cases were run to evaluate model performance under a constant heating regime. The initial conditions for each test were a uniform temperature gradient below the ML of 0.05°C/m, a ML depth of 40 m, a ML temperature of 10°C, and a wind speed of 5 m/s. Three heating cases were considered with surface heat fluxes of 125, 250, and 500 W/m$^2$. The simulations were run for 120 hours to approximate heating conditions applicable to the Great Lakes region.

For the 125-W/m$^2$ case, KLD had the deepest ML, followed by RT, RWG, and K. When the surface heat flux was increased to 250 W/m$^2$, the RWG, RT, and KLD models produced similar results, while K was significantly shallower. Under 500-W/m$^2$ heating the ML predicted by RT was 9 m, while RWG's was 8 m, KLD's was 6 m, and K's was a shallow 2 m. KLD showed the greatest absolute range in ML depth with a 20-m difference between the highest- and lowest-heating cases. The model sensitivity to different heating conditions decreased dramatically with the remaining models. RWG showed a 12-m range, RT showed a 9-m range, and K showed only a 2-m difference in ML depths.

The K model produced the shallowest ML in each case and the coolest SST under strong heating, and because of the nature of the diffusion equation it also produced the smoothest temperature profiles. Even at the lower heat flux, the K model did not technically produce an isothermal surface layer, and thus the ML depth is really an artifact of the way it has been defined. The temperature gradients in the surface layer tend toward a linear equilibrium profile, which is the commonly known response of the diffusion equation to constant diffusivities and to a constant heat flux boundary condition.

Model responses were most similar to one another under cooling conditions. Three different tests were made with sur-

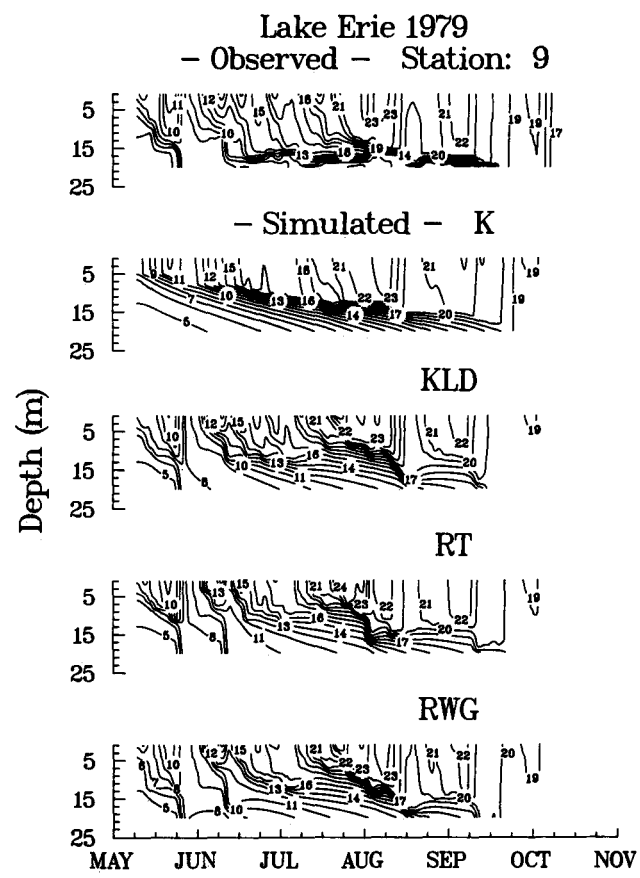


Fig. 4. Low-pass-filtered observed and simulated isotherms for station 9. Contour interval is 1°C.

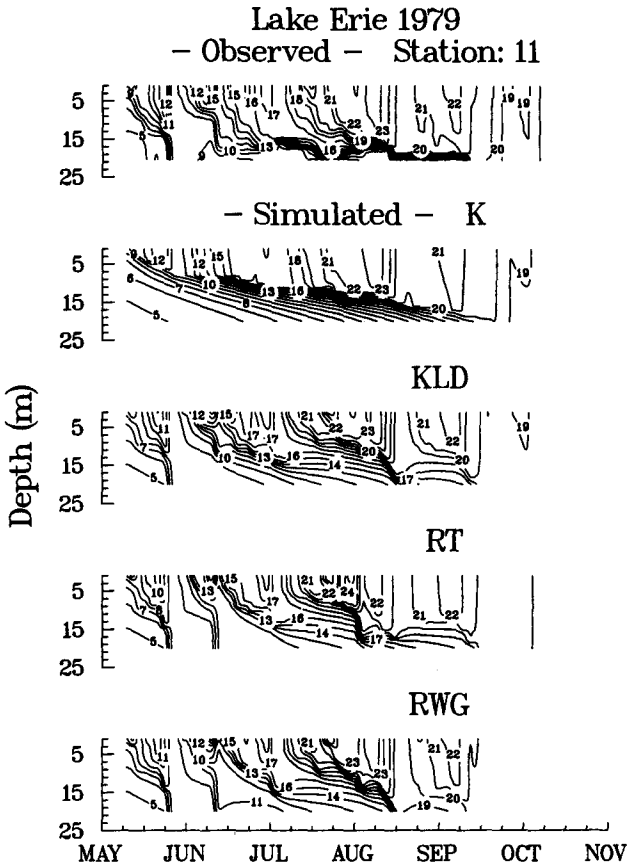


Fig. 5. Same as Figure 4 but for station 11.

face heat fluxes of −125, −250, and −500 W/m$^2$. The initial conditions were the same linear temperature gradient below the ML as before, a 5-m/s wind speed, a 15-m-deep ML, and a ML temperature of 20°C. Each test was run for 120 hours and the results are tabulated in Table 1. In all three cooling cases the final ML temperatures and depths were quite similar. During surface cooling periods the maximum difference in ML depths between any of the models is only 6 m. The close agreement between models suggests that convection driven by gravitational instabilities is dominating the model physics.

*Water Temperature and ML Depth Comparisons*

Figures 4–7 show observed and simulated isotherms for Lake Erie. The contour interval is 1°C and all isotherms were smoothed by low-pass filtering the data with a 96-hour period cutoff. In general, the Lake Erie data are seen as being weakly stratified in the upper 15 m of the water column through much of the season. The deeper bottom waters, though, show prolonged periods of intense stratification with temperature gradients in excess of 2°C/m. In the early part of the season the water column is weakly stratified until a strong storm passes near the end of May, mixing the entire water column to uniform temperature. By the end of June a strong thermocline is evident near the bottom, and it persists until mid-September when the lake is driven isothermal by convection resulting from surface cooling.

The thermal structures of stations 9, 11, and 21 appear to be very similar to one another, while station 19 differs from 9, 11, and 21 primarily in the bottom waters. Relative to the other stations, 19 is only weakly stratified until early July when the bottom waters begin showing strong temperature gradients. While 9, 11, and 21 show relatively lengthy periods of strong stratification, with near horizontal isotherms, station 19 shows a pronounced shallowing of the near-bottom thermocline in late July with its isotherms rising sharply toward the surface. The ML depth remains stable until early August and then is followed by a period of steady ML deepening much like that at the other stations.

The K model simulations of the Lake Erie data show little variation from station to station. Simulation of SST and the upper water column looks reasonable, while the general shape of the modeled isotherms at depth are poor compared to those observed. The simulated temperature field begins with a shallow ML which gradually deepens until the lake goes isothermal in mid to late September, and the isotherms show little to no evidence of storm-induced deepening.

At station 9 (Figure 4) the RT, KLD, and RWG models simulate the ML temperatures well. The late May storm-induced deepening appears to be well described by each of these models. Temperature gradients at depth are strong, with KLD, RT, and RWG showing more realism than K but not as much as is seen in the data.

The period of maximum stratification simulated by KLD, RT, and RWG for station 9 extends from mid-July to early August. All three models show steady ML deepening to occur over the first 2 weeks in August. By the second week in August the three models show similar deepening rates, as suggested by

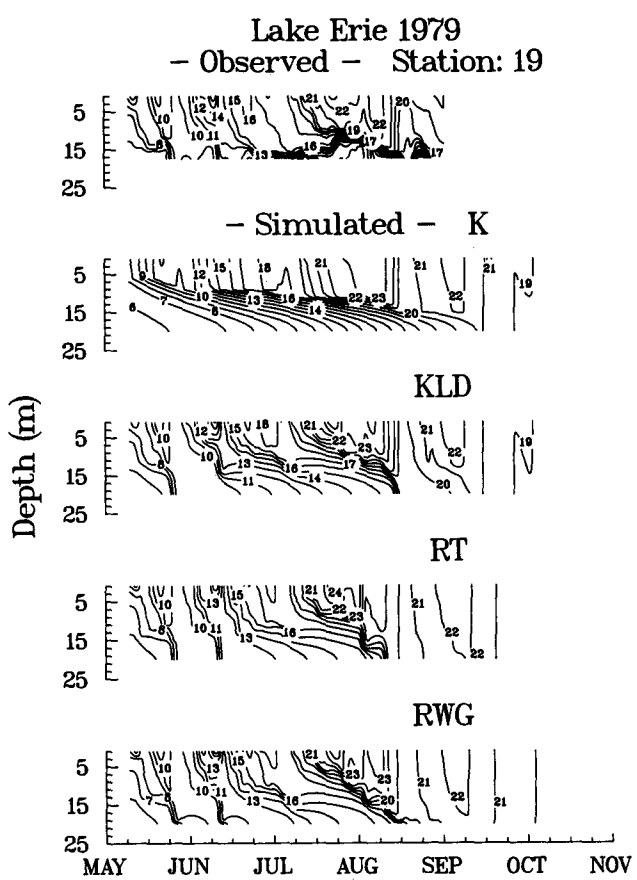


Fig. 6. Same as Figure 4 but for station 19.

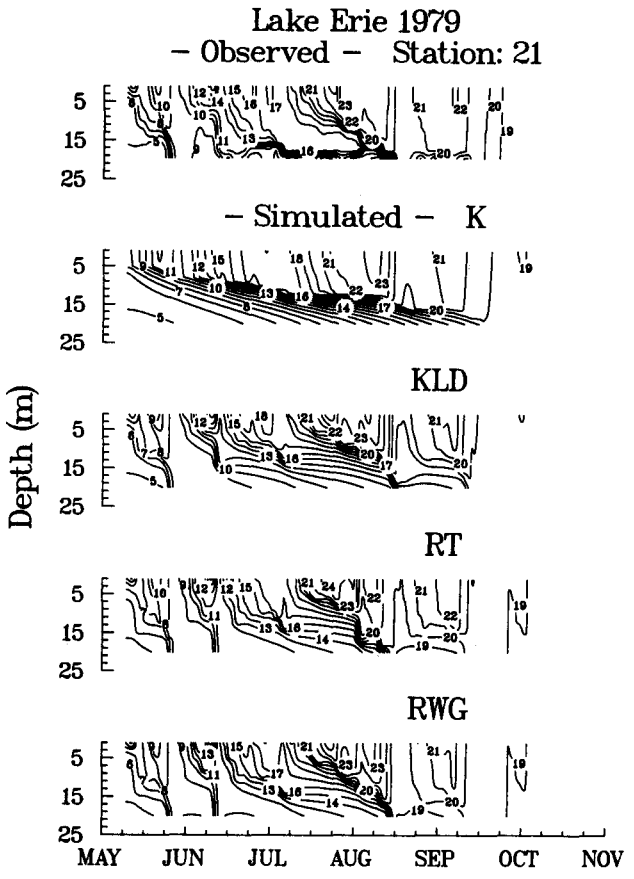


Fig. 7. Same as Figure 4 but for station 21.

the slope of the isotherms, pushing the ML to near bottom. This was followed by an increase in stratification at depth, with KLD and RT looking more like the data than RWG.

At station 11 (Figure 5), RWG showed less stratification at depth during July and August than it did at station 9. The ML deepening that occurred during mid-August drove the ML, in the RWG simulation, to the bottom, producing an isothermal water column. Neither RT nor KLD deepened to that degree, and thus they look more like the data and more like their simulations of station 9.

The KLD, RT, and RWG models simulated their weakest stratification of all stations at station 19 (Figure 6). The weaker stratification resulted in greater warming at depth during midsummer than was seen both elsewhere in the lake and in the data.

Compared to station 19, the degree of stratification simulated at station 21 (Figure 7) increased with the RT simulation, although the temperature gradients at depth during August were still somewhat weaker than those simulated at stations 9 and 11. The RWG and KLD simulations both look similar to their simulations at station 11. However, in this case RWG's simulation from mid-August on looks more like the data than KLD's. Namely, station 21 shows less stratification during this time period than is seen in the data at station 11. At 11, RWG underestimated the density stratification, while KLD did a better approximation of the thermal structure. At 21 the situation is reversed, and hence RWG looks more like the data, during this time period, than KLD. The RT simulation looks intermediary to those generated by it at 9 or 11 versus 19.

A clearer indication of overall model performance for the ML temperatures is seen in Table 2. The RMSEs between simulated and observed data were calculated at four different time scales which were selected on the basis of both the physical time scales governing lake dynamics and the practical time scales of interest associated with applied problems. The four time scales chosen for comparison were hourly, daily, weekly, and monthly. The RMSEs for the daily and longer-period time scales are calculated from low-pass-filtered data series with the appropriate cutoff frequencies. The RMSEs in Table 2 show little station-to-station variation, and they are approximately 1°C for all models at weekly and higher-frequency time scales. At monthly time scales the K model had the lowest RMSE at each station.

The predicted and observed ML depths are shown in Figure 8. For clarity the observed and simulated data have been low-pass filtered with a 24-hour cutoff period. From Figure 8 it is clear that the K model had the greatest difficulty tracking storm-induced deepening following the late May storm. The ML depths simulated by K are too shallow, in general, and

TABLE 2. RMSE Between Modeled and Observed Water Temperatures in Lake Erie

| | | RMSE, °C | | | |
|---|---|---|---|---|---|
| Station | Model | Hourly | Daily | Weekly | Monthly |
| 9 | K | (0.98) | (0.99) | (0.80) | (0.54) |
| | KLD | 1.07 | 1.07 | 0.99 | 0.84 |
| | RT | 1.03 | 1.03 | 0.90 | 0.69 |
| | RWG | 1.04 | 1.04 | 0.92 | 0.71 |
| 11 | K | 1.17 | 1.17 | 0.93 | (0.63) |
| | KLD | 1.23 | 1.22 | 1.12 | 0.97 |
| | RT | 1.11 | 1.10 | 0.96 | 0.77 |
| | RWG | (1.04) | (1.02) | (0.88) | 0.71 |
| 19 | K | 1.23 | 1.23 | 1.04 | (0.84) |
| | KLD | 1.27 | 1.26 | 1.18 | 1.09 |
| | RT | (1.10) | (1.09) | (1.02) | 0.96 |
| | RWG | 1.11 | 1.10 | (1.02) | 0.96 |
| 21 | K | 1.04 | 1.05 | (0.82) | (0.55) |
| | KLD | 1.14 | 1.13 | 1.04 | 0.90 |
| | RT | 1.04 | 1.02 | 0.93 | 0.82 |
| | RWG | (0.98) | (0.97) | 0.85 | 0.74 |

Water temperatures are at 1 m. Lowest RMSEs are in parentheses. The total number of observations made was 3675.

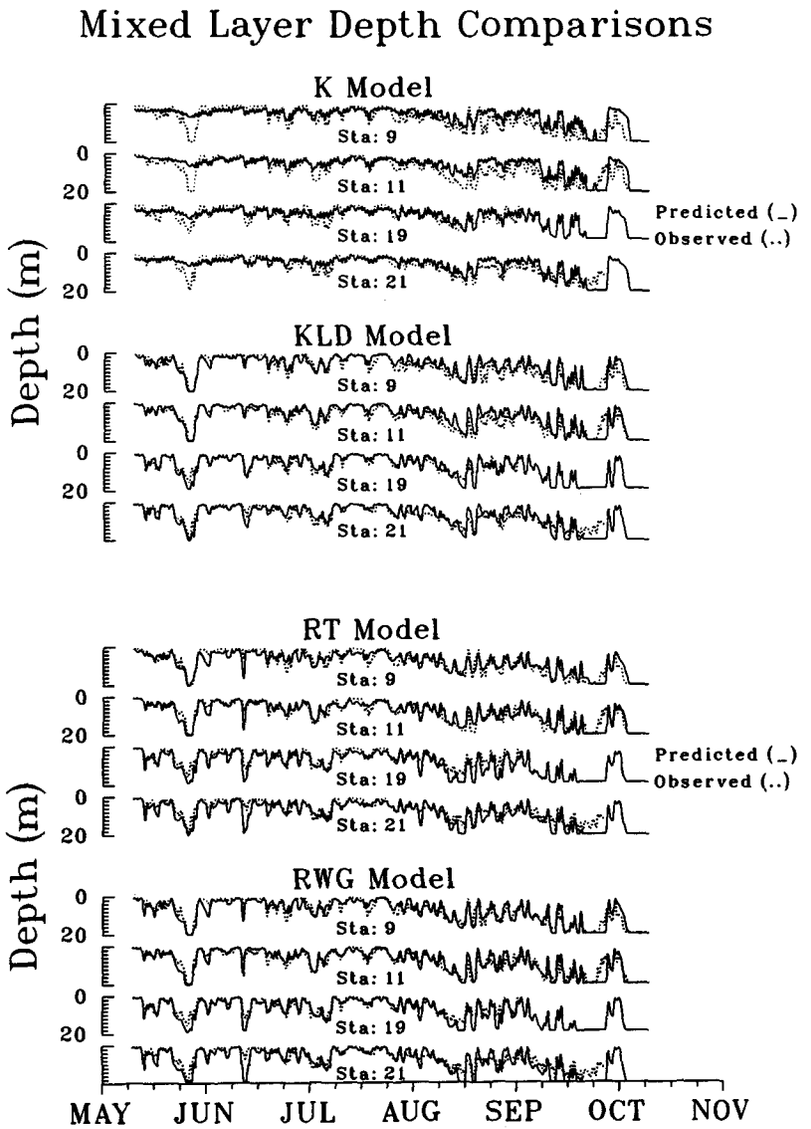


Fig. 8. Low-pass-filtered observed and simulated mixed layer depths.

the model is most successful during midsummer when the water column is strongly stratified and there is little temporal variability in $h$. The KLD, RT, and RWG models, though, were significantly more successful at tracking the ML depth, and in particular, each model was faithful in reproducing the collapse of the ML during the late May storm. However, the ML statistics in Table 3 show that no model clearly dominated in terms of skill (RMSE) nor in terms of coarse statistical measures (mean and variance). The RMSEs looked similar with respect to station-to-station and model-to-model variability, with the exception of K which had the largest RMSEs in general. In matching the ML depth variances, KLD was closest in value to real data at stations 11 and 19, RWG was closest at 9, and K was closest at 21. The best agreement between mean ML depths from model estimates versus data was shared by RT and KLD, with RT being the best at 9 and 11 and KLD at 19 and 21. RWG was nearly equal to RT in the mean ML depths at both 9 and 11 as well as in its RMSE behavior at all stations.

*Entrainment Rates and Their Spectra*

The episodic nature of ML deepening suggests that equally important as the model ability to simulate temperature and $h$ is the ability to simulate the correct entrainment rates $dh/dt$ at the appropriate frequencies. Entrainment rates, both observed and modeled, were estimated from hourly differences in the calculated values of the ML depth from data and from hourly averaged values from model simulation. Only positive or zero values of $dh/dt$ were considered.

Summary statistics for $dh/dt$ are shown in Table 4 from which several points emerge. First, the mean absolute error (MAE) and the RMSE show little model to model differences at each station. Second, the observed variance in $dh/dt$ is always underpredicted by each model. Third, the model-to-model differences in variance in $dh/dt$ are often quite large. Fourth, in general, the model-estimated mean entrainment rates are in fair agreement with those from data. Fifth, the K model best matches the observed mean entrainment rates in

TABLE 3. Predicted and Observed ML Depth Statistics Including RMSE for Lake Erie

| | Mean, m | | Variance, $m^2$ | | | RMSE, m | | | |
|---|---|---|---|---|---|---|---|---|---|
| Station | Observed | Predicted | Observed | Predicted | Model | Hourly | Daily | Weekly | Monthly |
| 9 | 8.3 | 6.5 | 44.0 | 30.2 | K | 4.8 | 4.0 | 3.1 | 3.0 |
| | | 7.4 | | 38.6 | KLD | (3.5) | 2.7 | 1.9 | 3.1 |
| | | (8.3) | | 33.1 | RT | (3.5) | (2.6) | 1.5 | 3.8 |
| | | 8.4 | | (44.1) | RWG | (3.5) | (2.6) | (1.4) | (2.6) |
| 11 | 8.7 | 6.5 | 39.9 | 31.6 | K | 4.8 | 4.1 | 3.3 | 3.0 |
| | | 7.3 | | (41.0) | KLD | (3.4) | 2.8 | 2.2 | 2.1 |
| | | (8.6) | | 39.0 | RT | (3.4) | (2.5) | 1.6 | 1.5 |
| | | 8.5 | | 48.2 | RWG | (3.4) | 2.6 | (1.4) | (1.3) |
| 19 | 5.8 | 5.3 | 20.3 | 13.1 | K | 3.6 | 2.6 | 1.5 | 1.6 |
| | | (5.6) | | (23.6) | KLD | (3.0) | (2.0) | (1.2) | (1.4) |
| | | 7.4 | | 30.2 | RT | 3.7 | 2.8 | 2.1 | 2.2 |
| | | 6.9 | | 33.9 | RWG | 3.6 | 2.7 | 1.9 | 1.9 |
| 21 | 7.0 | 6.1 | 28.0 | (24.7) | K | 4.2 | 3.0 | 2.3 | 1.9 |
| | | (6.9) | | 36.9 | KLD | (3.8) | (2.7) | (2.0) | (1.6) |
| | | 8.4 | | 38.3 | RT | 4.2 | 3.2 | 2.2 | 2.0 |
| | | 8.1 | | 45.4 | RWG | 4.5 | 3.4 | 2.3 | 2.0 |

Best model results are in parentheses.

all cases. Sixth, the RT model comes closest to reproducing observed variances in three out of four data comparisons.

At this point one might conclude that because the MAEs and RMSEs are similar, each model is equal in its skill to accurately simulate *dh/dt*. Furthermore, one might also conclude that because the K model showed the best agreement with the mean observed entrainment rates, it is therefore the best choice for modeling mixing in surface waters. This is wrong. The only way that selection could be defended is if the mean entrainment rate could explain most of the observed entrainment variability. This is not the case, as will be seen shortly by examining the spectral distribution of *dh/dt*.

Figures 9–12 show the observed and modeled spectral distribution of energy, coherency, and phase for entrainment in Lake Erie. The spectra were determined by standard techniques [*Jenkins and Watts*, 1968]. Data were first processed by removing the mean, followed by tapering the ends of the series with a split-cosine-bell data window, and then transformed with a fast Fourier transform, after *Claerbout* [1976], using a total of 256 lags. The relatively flat spectra seen in each figure resemble a white noise spectrum. This suggests that an approximately equal variability in *dh/dt* is present at all frequencies. The squared coherency and phase spectra also show the noisy and randomlike relationship between modeled and observed estimates of *dh/dt*. Yet useful information is still present.

First, over 90% of the variability in entrainment occurs at frequencies higher than 1 cpd. Second, although no model is coherent with the data, the RT model, followed by RWG, matches the observed entrainment energy level better than K or KLD.

## Discussion and Conclusions

The predictability of SST, as measured in terms of RMSE, was comparable to oceanic cases for KLD, RT, and RWG. For example, *Thompson* [1977] had a RMSE of approximately 0.5°C with his model in the Pacific Ocean. This compares favorably with the 1°C RMSEs seen in Lake Erie and is particularly encouraging since the temperature range in SST for Erie was much greater than the range *Thompson* [1976,

TABLE 4. Model Entrainment Statistics for Lake Erie

| | | *dh/dt*, m/h | | | | | |
|---|---|---|---|---|---|---|---|
| | | Observed | | Modeled | | | |
| Station | Model | Mean | Variance | Mean | Variance | MAE | RMSE |
| 9 | K | 0.37 | 1.37 | (0.27) | 0.19 | 0.48 | 1.20 |
| | KLD | | | 0.18 | 0.19 | 0.42 | 1.19 |
| | RT | | | 0.20 | (0.44) | 0.47 | 1.31 |
| | RWG | | | 0.22 | 0.34 | 0.47 | 1.23 |
| 11 | K | 0.32 | 0.67 | (0.27) | 0.18 | 0.41 | 0.87 |
| | KLD | | | 0.19 | 0.20 | 0.37 | 0.87 |
| | RT | | | 0.20 | 0.32 | 0.40 | 0.94 |
| | RWG | | | 0.21 | (0.36) | 0.42 | 0.97 |
| 19 | K | 0.52 | 2.27 | (0.30) | 0.16 | 0.63 | 1.54 |
| | KLD | | | 0.20 | 0.18 | 0.57 | 1.55 |
| | RT | | | 0.26 | (0.64) | 0.65 | 1.69 |
| | RWG | | | 0.24 | 0.41 | 0.62 | 1.60 |
| 21 | K | 0.47 | 1.66 | (0.29) | 0.19 | 0.57 | 1.32 |
| | KLD | | | 0.19 | 0.21 | 0.52 | 1.34 |
| | RT | | | 0.23 | (0.46) | 0.57 | 1.42 |
| | RWG | | | 0.24 | 0.42 | 0.58 | 1.42 |

Statistics are calculated from hourly data, and the best estimates are in parentheses.

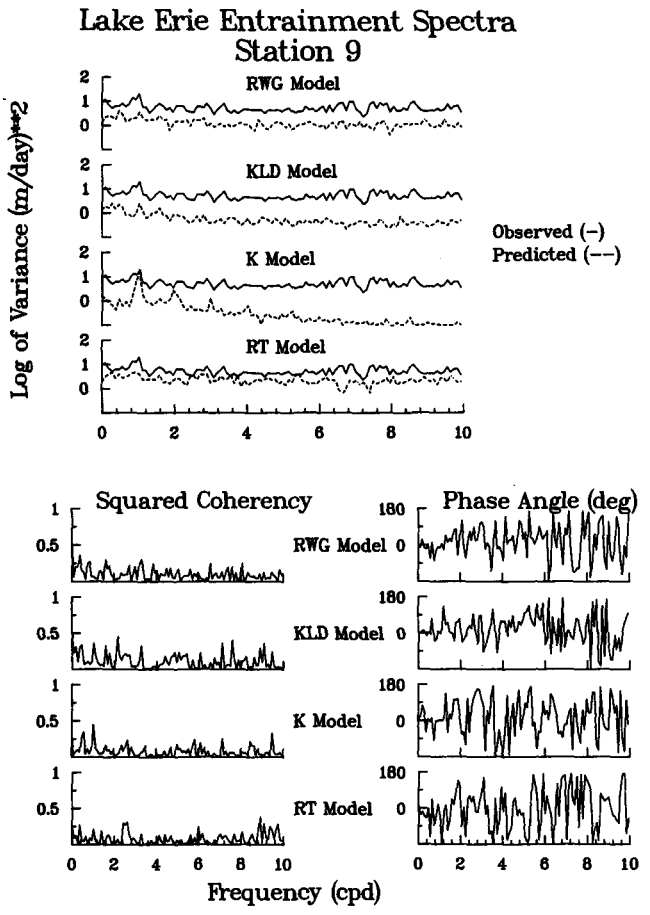


Fig. 9. Observed and modeled spectra of entrainment variance, squared coherency, and phase for station 9.

1977] encountered in his simulations, i.e., 7°–25°C versus 15°–25°C, respectively, and because the shallow depths of Lake Erie are in such sharp contrast to the depths of the oceanic applications. In fact, the 1°C RMSE the models generated in Erie is only about 0.3°C greater than the root-mean-square difference in the temperature data that exists between stations.

Overall, the model skills in reproducing the thermal structure in the upper regions of the water column were high. Attempts were made, though, to see if additional improvement was possible by identifying and then reducing potential model bias. Changes in the heat content and surface heat flux from both models and data were used to explore for bias. The heat content of the water column, as suggested by the data, was determined by integrating the temperature profile each hour that data were available. Next the heat flux was estimated by calculating the hourly rate of change in heat content. This quantity was then defined as the "observed" heat flux. The "predicted" heat flux was defined by the model-estimated heat flux across the air-water interface. If the heating process were one-dimensional, and both the models and data were perfect, then the observed and predicted heat fluxes would be identical. However, through low-pass filtering the observed and predicted heat fluxes, with various cutoff frequencies, it was revealed that the models, in general, tended to overpredict the observed heat flux by a nearly constant 20 W/m$^2$.

This apparent bias is only about 2% of the maximum summertime surface heat flux or about 10% of the mean annual signal. *Wyrtki and Uhrich* [1982] suggest that the uncertainty with heat inputs may range from 7 W/m$^2$ for long time scales to 20–30 W/m$^2$ for monthly episodes. Although the excess flux calculated herein is within these expectations, the long-term persistence of an error of this magnitude would lead to serious errors. Hence additional simulations were run with a constant 20 W/m$^2$ subtracted from the model-calculated surface heat flux. The results showed the predicted heat flux to be reduced only 2–3 W/m$^2$, and the RMSEs in SST changed little, suggesting that the 20-W/m$^2$ discrepancy in heat fluxes is not an accurate estimate of model bias. Also, these results further suggest that the feedback mechanism between air and surface water temperatures appears to be strong enough that the models are not overly sensitive to small changes in the surface heat flux during summer stratification.

*Price et al.* [1978] noted that modeling efforts where the entrainment rate is scaled according to $U_*$ and according to $\Delta V$ have both been successful, but that the success of either scale was due more to the nature of the data than to an accurate scaling of the physics. Namely, $U_*$ can work well except where storm-induced deepening is concerned, in which case $\Delta V$ is the proper scale. This work also supports these conclusions as suggested by the higher and better estimates of entrainment energy made by the two models, RT and RWG, that use the $\Delta V$ scaling.

Estimates of the shear velocity $\Delta V$ at the mixed layer base were made in both RT and RWG by assuming the mixed layer flow to be composed of wind-forced pure inertial motions and

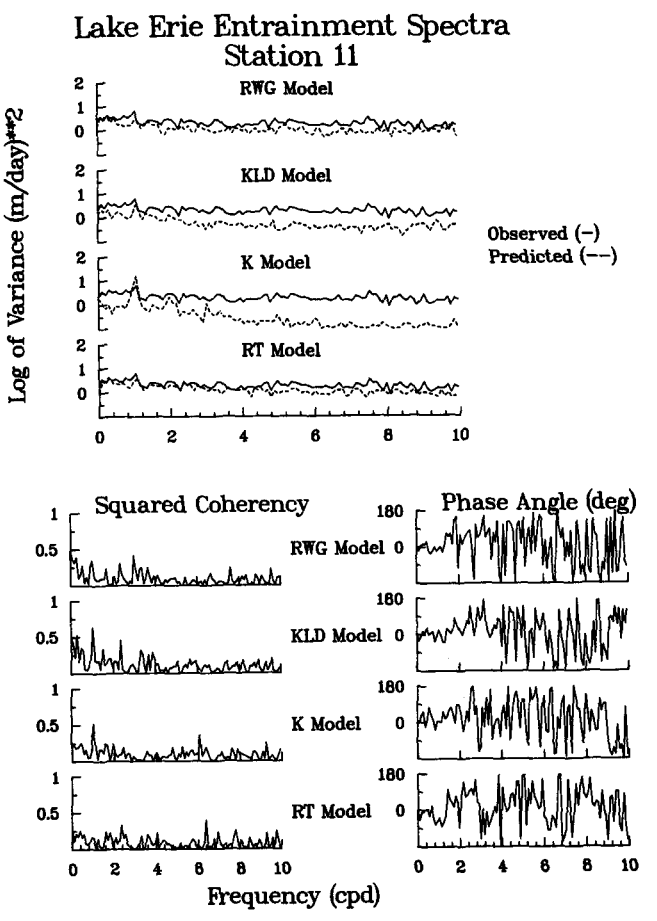


Fig. 10. Same as Figure 9 but for station 11.

a no-flow condition to exist in the bottom waters [*Thompson*, 1976]. Hence the shear source was presumed to originate from inertial currents only. In Lake Erie the flow field is more complicated than depicted here, yet works by *Ivey and Patterson* [1984] and *Boyce and Chiocchio* [1987] lend credence to the approach used here. Ivey and Patterson accurately simulated Lake Erie temperature profiles with a one-dimensional model after *Niiler* [1975], whereby estimates of $\Delta V$ were augmented by data from near-bottom mounted current meters. Similarly, spectral calculations of Lake Erie temperatures and current meter data by *Boyce and Chiocchio* [1987] showed the dominant spectral peak to be at the local inertial frequency, and during periods of strong inertial motion Boyce and Chiocchio observed the maximum current velocities lying just above the seasonal thermocline with a bottom flow counter to that in the surface-mixed layer. Boyce and Chiocchio were successful in using a one-dimensional diagnostic model to describe the offshore vertical current structure. In their model they assumed that a local balance existed between the surface Ekman transport and the pressure gradient driven bottom flow, such that no net transport occurred in the vertically integrated flow. In our work, no attempt was made to account for the bottom flow. Under this scenario our method of estimating $\Delta V$ should, in general, underestimate the true current shear. The spectral analyses of $dh/dt$ support this interpretation, but they also suggest that some estimate of $\Delta V$ is desirable. Therefore the simple Ekman dynamics calculations made here are useful for estimating the shear source contribution to mixed layer deepening. If better estimates of the thermal structure at depth are desired, then better estimates of $\Delta V$ will be necessary.

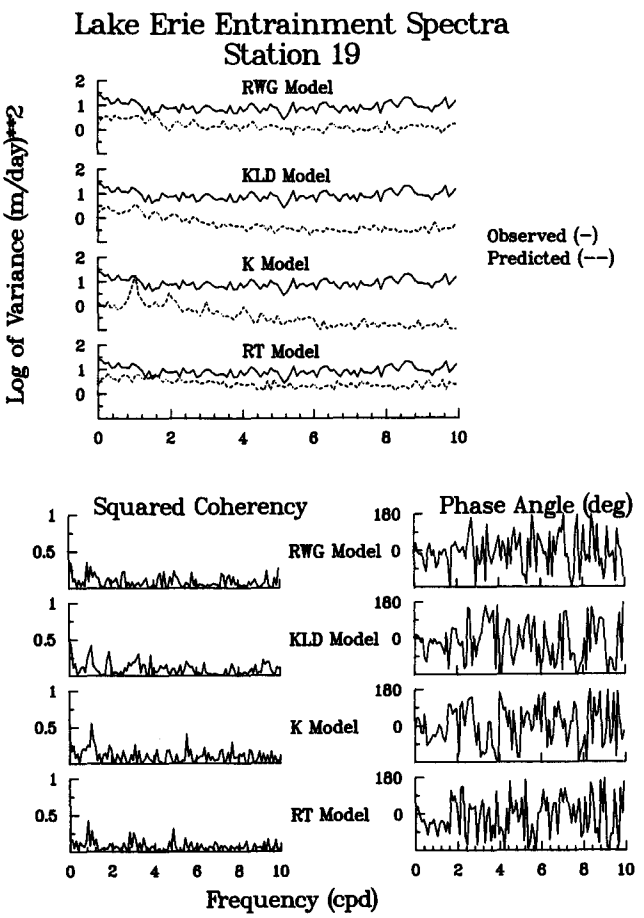


Fig. 11. Same as Figure 9 but for station 19.

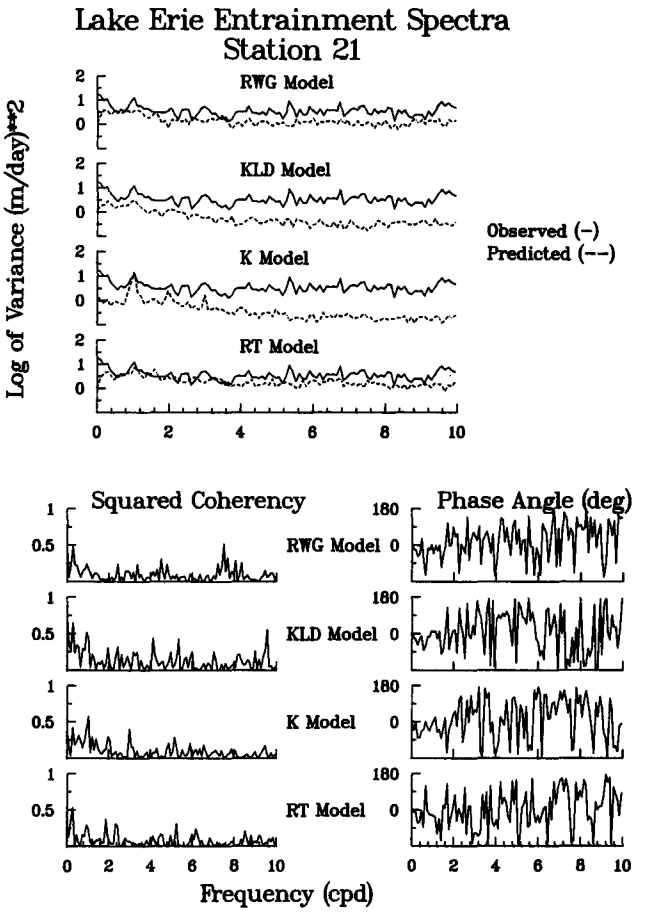


Fig. 12. Same as Figure 9 but for station 21.

Several points from this work are noteworthy:

1. The SST was simulated, in general, with equal accuracy in terms of the RMSE, by each model at time scales ranging from hourly to monthly.

2. Three of the models examined, KLD, RT, and RWG, were successful in accurately tracking the ML depth in spite of the shallow water environment of Lake Erie. These models showed little bias between the modeled and observed mean ML depths and tracked the storm-induced deepening of the ML with high accuracy. The K model failed to simulate this storm event and consistently underpredicted the mean ML depth at each station. Whatever success was achieved by the K model appears to stem from convective mixing rather than from a meaningful mixing parameterization. This was suggested by the modeled variability in $dh/dt$ and $h$ being concentrated at the diurnal frequency, the same frequency dominating in the variance distribution of the surface heat flux.

3. Before any hard decision is made as to the appropriateness of a model, the intended application must be clear. For example, if only the SST is desired, then as previously mentioned, any one of the models is satisfactory. However, if vertical mixing is an important part of the intended application, or equivalently if diurnal physical processes are of interest, then the model ability to simulate both the ML depth and the energy level associated with entrainment $dh/dt$ becomes crucial.

While three of the models, KLD, RT, and RWG, were satisfactory in simulating the ML depth, only two of the models, RT and RWG were satisfactory in simulating the energy level associated with $dh/dt$. These two models showed the best agreement between modeled and observed data in matching the energy levels of $dh/dt$ as inferred from the entrainment spectra. This agreement suggests that the $\Delta V$ entrainment scaling plays a critical role in the cycling of shallow depth mixed layers.

*Acknowledgments.* The data used in this study were a pleasure to work with because of their extensive coverage and high quality and were generously provided to us from two sources. First, we thank Jim Bull of the National Water Research Institute for providing the meteorological data from their Lake Erie field program, and second, we thank Jim Saylor and Gerry Miller of the Great Lakes Environmental Research Laboratory for the use of their water temperature data. We are also grateful to Paul Martin of the Naval Ocean Research and Development Activity for his thorough and thoughtful review of the initial stages of this work and for providing us the RWG computer code, and to Rory Thompson for his careful review of the preliminary results and for the subsequent mistakes he discovered.

## References

Adamec, D., R. L. Elsberry, R. W. Garwood, Jr., and R. L. Haney, An embedded mixed-layer-ocean circulation model, *Dyn. Atmos. Oceans*, *6*, 69–96, 1981.

Allender, J. H., and J. H. Saylor, Model and observed circulation throughout the annual temperature cycle of Lake Michigan, *J. Phys. Oceanogr.*, *9*, 573–579, 1979.

Batchelor, G. K., and A. A. Townsend, Turbulent diffusion, in *Surveys in Mechanics*, edited by G. K. Batchelor and R. M. Davies, pp. 352–399, Cambridge University Press, New York, 1956.

Bennett, J. R., A three-dimensional model of Lake Ontario's summer circulation, *J. Phys. Oceanogr.*, *7*, 591–601, 1977.

Bennett, J. R., The circulation of large lakes, in *Upwelling Ecosystems*, edited by R. Boje and M. Tomczak, pp. 223–234, Springer-Verlag, New York, 1978.

Boyce, F. M., Some aspects of Great Lakes physics of importance to biological and chemical processes, *J. Fish. Res. Board Can.*, *31*, 689–730, 1974.

Boyce, F. M., and F. Chiocchio, A study of inertial frequency current oscillations in the central basin of Lake Erie, *J. Great Lakes Res.*, *13*, 542–558, 1987.

Businger, J. A., J. C. Wyngaard, Y. Izumi, and E. F. Bradley, Flux-profile measurements in the atmospheric surface layer, *J. Atmos. Sci.*, *28*, 181–189, 1971.

Claerbout, J. F., *Fundamentals of Geophysical Data Processing: With Applications to Petroleum Prospecting*, 274 pp., McGraw-Hill, New York, 1976.

Clancy, R. M., and K. D. Pollack, A real-time synoptic ocean thermal analysis/forecast system, *Prog. Oceanogr.*, *12*, 383–424, 1983.

Cotton, G. F., ARL models of global solar radiation, Hourly solar radiation—Surface Meteorological Observations, Solmet final report, vol. 2, pp. 165–184, Natl. Clim. Center Asheville, N. C., 1979.

Cushman-Roisin, B., Deepening of the wind-mixed layer: A model of the vertical structure, *Tellus*, *33*, 564–582, 1981.

Davis, R. E., Oceanic property transport, Lagrangian particle statistics, and their prediction, *J. Mar. Res.*, *41*, 163–194, 1983.

Deardorff, J. W., A three-dimensional numerical investigation of the idealized planetary boundary layer, *Geophys. Fluid. Dyn.*, *1*, 377–410, 1970.

Denman, K. L., A time-dependent model of the upper ocean, *J. Phys. Oceanogr.*, *3*, 173–184, 1973.

Denman, K. L., and M. Miyake, Upper layer modification at ocean station Papa: Observations and simulation, *J. Phys. Oceanogr.*, *3*, 185–196, 1973.

De Ruijter, W. P. M., Frontogenesis in an advective mixed-layer model, *J. Phys. Oceanogr.*, *13*, 487–495, 1983.

De Szoeke, R. A., On the effects of horizontal variability of wind stress on the dynamics of the ocean mixed layer, *J. Phys. Oceanogr.*, *10*, 1439–1454, 1980.

Elsberry, R. L., T. S. Fraim, and R. N. Trapnell, Jr., A mixed layer model of the oceanic thermal response to hurricanes, *J. Geophys. Res.*, *81*, 1153–1162, 1976.

Garwood, R. W., Jr., An oceanic mixed layer capable of simulating cyclic states, *J. Phys. Oceanogr.*, *7*, 455–468, 1977.

Garwood, R. W., Jr., Air-sea interaction and dynamics of the surface mixed layer, *Rev. Geophys.*, *17*, 1507–1524, 1979.

Garwood, R. W., and N. T. Camp, Comments on "Climatological numerical models of the surface mixed layer of the ocean," *J. Phys. Oceanogr.*, *7*, 469–470, 1977.

Gill, A. E., and J. S. Turner, A comparison of seasonal thermocline models with observation, *Deep Sea Res.*, *23*, 391–401, 1976.

Hoeber, H., Eddy thermal conductivity in the upper 12 m of the tropical Atlantic, *J. Phys. Oceanogr.*, *2*, 303–304, 1972.

Ivanoff, A., Oceanic absorption of solar energy, *Modeling and Prediction of the Upper Layers of the Ocean*, edited by E. B. Kraus, pp. 47–72, Pergamon, Elmsford, New York, 1977.

Ivey, G. N., and J. C. Patterson, A model of vertical mixing in Lake Erie in summer, *Limnol. Oceanogr.*, *29*, 553–563, 1984.

Jacobsen, J. P., Beitrag zur hydrographie der danischen Gewasse, *Med. Komm. Havunders. Ser. Hydrogr.*, *2*, 1–94, 1913.

Jenkins, G. M., and D. G. Watts, *Spectral Analysis and Its Applications*, 525 pp., Holden Day, Oakland, Calif., 1968.

Kent, R. E., and D. W. Pritchard, A test of mixing length theories in a coastal plain estuary, *J. Mar. Res.*, *18*, 62–72, 1959.

Kraus, E. B., and J. S. Turner, A one-dimensional model of the seasonal thermocline, part II, *Tellus*, *19*, 98–105, 1967.

Kundu, P. K., A numerical investigation of mixed-layer dynamic, *J. Phys. Oceanogr.*, *10*, 220–236, 1980.

Le Saos, J. P., and V. Mariette, Observation et simulation de l'évolution de la couche superficielle de l'ocean, *Oceanol. Acta*, *4*, 117–128, 1981.

Martin, P. J., Simulation of the mixed layer at OWS November and Papa with several models, *J. Geophys. Res.*, *90*, 903–916, 1985.

McCormick, M. J., and D. Scavia, Calculation of vertical profiles of lake-averaged temperature and diffusivity, in lakes Ontario and Washington, *Water Resour. Res.*, *17*, 305–310, 1981.

Mellor, G. L., and P. A. Durbin, The structure and dynamics of the ocean surface mixed layer, *J. Phys. Oceanogr.*, *5*, 718–728, 1975.

Mellor, G. L., and T. Yamada, A hierarchy of turbulence closure models for planetary boundary layers, *J. Atmos. Sci.*, *31*, 1791–1806, 1974.

Mellor, G. L., and T. Yamada, Development of a turbulence closure model for geophysical fluid problems, *Rev. Geophys.*, *20*, 851–875, 1982.

Moen, J., A review of one-dimensional oceanic mixed-layer models, *Rep. SR-47*, 50 pp., N. Atl. Treaty Organ., SACLANT ASW Res. Centre, San Bartolomeo, Italy, 1981.

Mortimer, C. H., Lake hydrodynamics, *Mitt. Int. Ver. Theor. Angelo. Limnol.*, *20*, 124–197, 1974.

Munk, W. H., and E. R. Anderson, Notes on a theory of the thermocline, *J. Mar. Res.*, *7*, 276–295, 1948.

Niiler, P. P., Deepening of the wind-mixed layer, *J. Mar. Res.*, *33*, 405–422, 1975.

Niiler, P. P., and E. B. Kraus, One-dimensional models of the upper ocean, in *Modeling and Prediction of the Upper Layers of the Ocean*, edited by E. B. Kraus, pp. 143–172, Pergamon, Elmsford, New York, 1977.

Oort, A. H., and A. Taylor, On the kinetic energy spectrum near the ground, *Mon. Weather Rev.*, *97*, 623–636, 1969.

Pacanowski, R. C., and S. G. H. Philander, Parameterization of vertical mixing in numerical models of tropical oceans, *J. Phys. Oceanogr.*, *11*, 1443–1451, 1981.

Pickett, R. L., and L. R. Herche, A simple density equation for Great Lakes waters, paper presented at the 27th Conference on Great Lakes Research, Brock Univ., St. Catherines, Ont., Canada, May 1–3, 1984.

Pinsak, A. P., and G. K. Rodgers, Energy balance, in *IFYGL—The International Field Year for the Great Lakes*, edited by E. J. Aubert and T. L. Richards, pp. 169–197, Great Lakes Environmental Research Laboratory, National Oceanographic and Atmospheric Administration, Ann Arbor, Mich., 1981.

Pollard, R. T., P. B. Rhines, and R. O. R. Y. Thompson, The deepening of the wind-mixed layer, *Geophys. Fluid Dyn.*, *3*, 381–404, 1973.

Price, J. F., C. N. K. Mooers, and J. C. Van Leer, Observation and simulation of storm-induced mixed-layer deepening, *J. Phys. Oceanogr.*, *8*, 582–599, 1978.

Roberts, P. H., Analytical theory of turbulent diffusion, *J. Fluid Mech.*, *11*, 257–283, 1961.

Saylor, J. H., and G. S. Miller, Investigation of the currents and density structure of Lake Erie, *Tech. Memo., ERL GLERL-49*, 80 pp., Natl. Oceanogr. and Atmos. Admin., Ann Arbor, Mich., 1983.

Schwab, D. J., Simulation and forecasting of Lake Erie storm usage, *Mon. Weather Rev.*, *106*, 1476–1487, 1978.

Schwab, D. J., J. R. Bennett, and A. T. Jessup, A two-dimensional lake circulation modeling system, *Tech. Memo., ERL GLERL-38*, 79 pp., Natl. Oceanogr. and Atmos. Admin., Ann Arbor, Mich., 1981.

Simons, T. J., Verification of numerical models of Lake Ontario, III, Long term heat transports, *J. Phys. Oceanogr.*, *6*, 372–378, 1976.

Stevenson, J. W., On the effect of dissipation on seasonal thermocline models, *J. Phys. Oceanogr.*, *9*, 57–64, 1979.

Sundaram, T. R., and R. G. Rehm, The seasonal thermal structure of deep temperate lake, *Tellus*, *25*, 157–167, 1973.

Taylor, G. I., Effect of variation in density on the stability of superposed streams of fluid, *Proc. R. Soc. London, Ser. A.*, *132*, 499–523, 1931.

Thompson, R. O. R. Y., Climatological numerical models of the surface mixed layer of the ocean, *J. Phys. Oceanogr.*, *6*, 496–503, 1976.

Thompson, R. O. R. Y., Reply to comments on "Climatological numerical models of the surface mixed layer of the ocean," *J. Phys. Oceanogr.*, *7*, 470–471, 1977.

Thompson, R. O. R. Y., A reinterpretation of the entrainment process in some laboratory experiments, *Dyn. Atmos. Oceans*, *4*, 45–55, 1979.

Walters, R. A., G. F. Carey, and D. F. Winter, Temperature computation for temperate lakes, *Appl. Math. Model.*, *2*, 41–48, 1978.

Woods, J. D., Parameterization of unresolved motions, in *Modeling and Prediction of the Upper Layers of the Ocean*, edited by E. B. Kraus, pp. 118–142, Pergamon, Elmsford, New York, 1977.

Wyrtki, K., The average annual heat balance of the North Pacific Ocean and its relation to ocean circulation, *J. Geophys. Res.*, *70*, 4547–4559, 1965.

Wyrtki, K., and L. Uhrich, On the accuracy of heat storage computations, *J. Phys. Oceanogr.*, *12*, 1411–1416, 1982.

Zeman, Q., and J. L. Lumley, Modeling buoyancy driven mixed layers *J. Atmos. Sci.*, *33*, 1974–1988, 1976.

M. J. McCormick, Great Lakes Environmental Research Laboratory, NOAA, 2205 Commonwealth Blvd., Ann Arbor, MI 48104.

G. A. Meadows, Department of Naval Architecture and Marine Engineering, University of Michigan, Ann Arbor, MI 48109.

(Received September 17, 1987;
accepted January 18, 1988.)